Journal of Sound and Vibration (1999) **227**(4), 735–748
Article No. jsvi.1999.2381, available online at http://www.idealibrary.com on IDEAL®

AN EFFICIENT METHOD FOR SOUND TRANSMISSION IN NON-UNIFORM CIRCULAR DUCTS

M. UTSUMI

Machine Element Department, Research Institute, Ishikawajima-Harima Heavy Industries Company Ltd., 3-1-15 *Toyosu, Koto-ku, Tokyo* 135-0061, *Japan*

(*Received* 24 *November* 1998, *and in final form* 4 *May* 1999)

An efficient method is presented in this paper for predicting the reflection and transmission coefficients of acoustic waves in ducts at the location of a continuous variation in cross-sectional area. Conventional numerical methods yield high dimensionality in the resulting numerical problem due to segmentation of the non-uniform section into a number of subsections. This paper shows that an ingenious application of spherical coordinates according to the geometry of the non-uniform section enables us to determine analytically the system of characteristic functions for various profiles of the non-uniform portion. This system of characteristic functions can be used as a complete set to express the solution over the non-uniform region, so that the numerical problem to be solved is of a much lower dimension than that yielded by conventional numerical methods. A technique to render the characteristic functions independent of the frequency is also explained to keep the computation time short. The present method is applicable to non-plane wave modes of propagation by virtue of the use of standard three-dimensional curvilinear co-ordinates.

1. INTRODUCTION

Calculation of reflection and transmission coefficients in ducts with a change in cross-sectional area is an important topic in acoustics. There are many practical situations where sound is propagated in such non-uniform ducts. For ducts having discontinuous changes in cross-sectional area, an analytical method can be applied [1], since analytical expressions for the characteristic functions constituting a solution to the wave equation are available over the region under consideration. The remaining work uses conventional Fourier expansion techniques to satisfy the condition of continuity at the discontinuities for the sound pressure and the fluid particle velocity. However, for ducts with continuously varying cross-sectional area, such an analytical solution is not available except for the case of the plane wave mode of propagation through linearly tapered ducts. In such cases, numerical methods have to be used, such as the method of weighted residuals [2–4] and the finite element method [5, 6], as well as perturbation methods like the ones described in the reference material [7, 8]. An alternative approach is a computation scheme used in the reference material [9–11]. This method represents a non-uniform duct with a series of stepped uniform ducts and systematically accounts for

0022-460X/99/440735 + 14 $30.00/0

the reflection and transmission process which occurs at the intersection of the stepped elements. These conventional methods yield a high dimensionality in the resulting numerical problem due to segmentation of the duct into many subsections or require an iterative calculation to obtain reasonably accurate results.

The purpose of this paper is to report a more efficient analytical method, which requires neither segmentation nor iterative calculation. Basically, we applied spherical co-ordinates according to the geometry of the non-uniform section, thus enabling us to determine analytically the system of characteristic functions for various profiles of the non-uniform portion of the duct. This system of characteristic functions can be used as a complete set to express the solution over the non-uniform region, so that the resulting numerical problem is of much lower dimension than that yielded by conventional numerical methods. Furthermore, the present method is applicable to non-plane wave modes of propagation by virtue of the use of standard three-dimensional curvilinear co-ordinates.

2. SOLUTION METHOD

2.1. COMPUTATIONAL MODEL

The geometry is defined in Figure 1, where two semi-infinite uniform duct sections are joined by a non-uniform transition section of length L. The side wall of

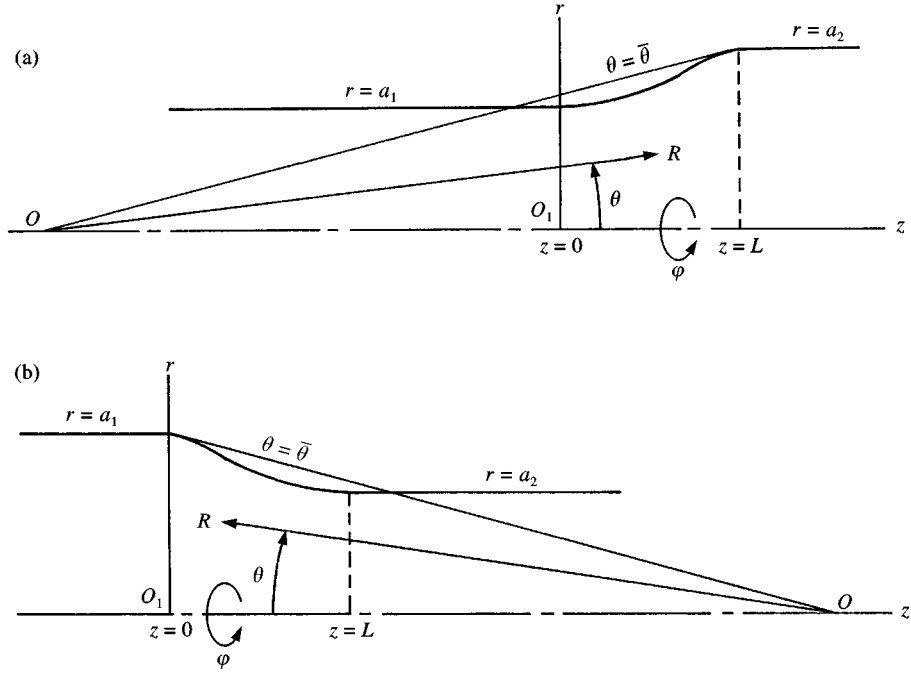

Figure 1. Computational model and co-ordinate systems (diverging (a) and converging (b) tapered transition sections).

the duct is assumed to be rigid for all the sections. The cylindrical co-ordinates r, φ and z are used to express the solution in the uniform sections $z \leqslant 0$ and $L \leqslant z$, while the spherical co-ordinates R, θ and φ are introduced to determine analytically the characteristic functions for the non-uniform portion $0 \leqslant z \leqslant L$. The origin O of the spherical co-ordinates is chosen as the apex of the cone whose side wall is tangent to the duct wall at the location having the largest cross-section. Such a use of the spherical co-ordinates is effective for geometries of the non-uniform portion satisfying the following conditions:

(1) The cross-sectional area increases or decreases monotonically with z.
(2) The side wall is not parallel to the z-axis at $z = L$ or $z = 0$ for the diverging (Figure 1(a)) or converging (Figure 1(b)) cases respectively.
(3) The region $0 \leqslant \theta \leqslant \bar{\theta}$ absorbs completely the non-uniform portion.

If condition (2) is not satisfied, the origin O tends towards minus or plus infinity and $\bar{\theta} \to 0$. This problem can be solved by slightly changing the position from which the tangent of the duct wall is drawn, such that $\bar{\theta}$ is a small non-zero value, i.e., 1°.

The sound pressure p in the uniform sections must satisfy the wave equation

$$\frac{\partial^2 p}{\partial t^2} = c^2\left(\frac{\partial^2 p}{\partial r^2} + \frac{1}{r}\frac{\partial p}{\partial r} + \frac{1}{r^2}\frac{\partial^2 p}{\partial \varphi^2} + \frac{\partial^2 p}{\partial z^2}\right) \tag{1}$$

subject to the boundary conditions

$$\frac{\partial p}{\partial r} = 0 \quad \text{for } r = a_1, \quad z \leqslant 0, \tag{2}$$

$$\frac{\partial p}{\partial r} = 0 \quad \text{for } r = a_2, \quad L \leqslant z, \tag{3}$$

where c is the speed of sound. The solution to equations (1)–(3) can be obtained by mathematical procedures described in references [1, 12] and are expressed as

$$p^{(I)} = C_{1mv}\mathrm{J}_m(\mu_{1mv}r)\exp(-\mathrm{i}k_{1mv}z)\cos m\varphi \exp(\mathrm{i}\omega t) \quad (z \leqslant 0), \tag{4}$$

$$p^{(R)} = \sum_{n=n_{min}}^{n_{max}} C_{2mn}\mathrm{J}_m(\mu_{1mn}r)\exp(\mathrm{i}k_{1mn}z)\cos m\varphi \exp(\mathrm{i}\omega t) \quad (z \leqslant 0), \tag{5}$$

$$p^{(T)} = \sum_{n=n_{min}}^{n_{max}} C_{3mn}\mathrm{J}_m(\mu_{2mn}r)\exp\{\mathrm{i}k_{2mn}(z-L)\}\cos m\varphi \exp(\mathrm{i}\omega t) \quad (z \geqslant L) \tag{6}$$

with

$$(k_{1mn})^2 = \{\omega^2 - (c\mu_{1mn})^2\}/c^2, \tag{7}$$

$$(k_{2mn})^2 = \{\omega^2 - (c\mu_{2mn})^2\}/c^2, \tag{8}$$

$$n_{min} = 0 \text{ (for } m = 0), \qquad n_{min} = 1 \text{ (for } m \geqslant 1), \tag{9}$$

where $p^{(I)}$, $p^{(R)}$ and $p^{(T)}$ represent the incident, reflected and transmitted waves respectively; C_{1mv}, C_{2mn} and C_{3mn} are complex constants; J_m is the Bessel function of the first kind of order m; μ_{1mn} and μ_{2mn} are the nth roots of $J_m(\mu a_1) = 0$ and $J_m(\mu a_2) = 0$ respectively; i is the imaginary unit; and ω is the angular frequency of interest. Note that the following constants

$$\mu_{100} = \mu_{200} = 0 \tag{10}$$

are defined such that equations (4)–(6) include the plane wave mode, for which sound pressure is constant throughout the cross-section of the duct.

The resulting task, then, is to determine the reflection and transmission coefficients for a prescribed mode (m, v) of the incident wave, so that $p^{(I)}$ (equation (4)) includes the mode (m, v) alone. However, $p^{(R)}$ and $p^{(T)}$ are expressed in terms of the superposition of many modes $(n = n_{min}, \ldots, n_{max})$ to satisfy the condition of continuity at $z = 0$ and $z = L$ by the Galerkin method later. Note that summation for the circumferential wave number m is not necessary here since the three sections $z \leqslant 0$, $0 \leqslant z \leqslant L$ and $L \leqslant z$ are coaxial. The summation over n in equations (5) and (6) can be physically explained by the fact that the divergence or convergence, under a model excitation with mode (m, v), will generate reflections and transmissions following a series of radial modes having the same circumferential index m.

The sound pressure P in the non-uniform portion satisfies the wave equation expressed in spherical co-ordinates:

$$\frac{\partial^2 P}{\partial t^2} = c^2\left(\frac{\partial^2 P}{\partial R^2} + \frac{2}{R}\frac{\partial P}{\partial R} + \frac{1}{R^2}\frac{\partial^2 P}{\partial \theta^2} + \frac{\cot\theta}{R^2}\frac{\partial P}{\partial \theta} + \frac{1}{R^2\sin^2\theta}\frac{\partial^2 P}{\partial \varphi^2}\right). \tag{11}$$

The solution of equation (11) must be expressed by a linear combination of characteristic functions whose orthogonality is satisfied within the range $0 \leqslant \theta \leqslant \bar{\theta}$. Since $\bar{\theta} < \pi/2$ (see Figure 1), such orthogonality cannot be satisfied by the widely used Legendre polynomials. This is the reason why the characteristic functions must be derived anew here. We assume a solution in terms of separated variables, i.e.,

$$P(R, \theta, \varphi, t) = F(R)\Theta(\theta)\cos m\varphi \, \mathrm{e}^{\mathrm{i}\omega t}. \tag{12}$$

Substitution of equation (12) into equation (11) gives

$$\frac{\mathrm{d}^2 F}{\mathrm{d}R^2} + \frac{2}{R}\frac{\mathrm{d}F}{\mathrm{d}R} + \left(k^2 - \frac{\lambda}{R^2}\right)F = 0, \tag{13}$$

$$\frac{\mathrm{d}^2 \Theta}{\mathrm{d}\theta^2} + \cot\theta\frac{\mathrm{d}\Theta}{\mathrm{d}\theta} + \left(\lambda - \frac{m^2}{\sin^2\theta}\right)\Theta = 0, \tag{14}$$

where k is the wave number given by

$$k = \omega/c \tag{15}$$

and λ denotes a characteristic value to be determined later. The new variables

$$u = kR, \quad G(u) = u^{1/2} F(R) \tag{16}$$

transform equation (13) into the Bessel equation of order $\sqrt{\lambda + 0{\cdot}25}$ with respect to G. Hence, the solution F can be expressed by a linear combination of the following two independent solutions:

$$F_1(R) = (kR)^{-1/2} \mathrm{J}_{\sqrt{\lambda+0{\cdot}25}}(kR), \qquad F_2(R) = (kR)^{-1/2} \mathrm{J}_{-\sqrt{\lambda+0{\cdot}25}}(kR). \tag{17}$$

On the other hand, equation (14) is solved for the boundary condition

$$\frac{\mathrm{d}\Theta}{\mathrm{d}\theta} = 0 \quad \text{at } \theta = \bar{\theta}. \tag{18}$$

This can be derived by considering the limit $\theta \to \bar{\theta}$ of the boundary condition on the duct wall

$$\frac{\partial P}{\partial N} = 0 \tag{19}$$

through the following procedures. From equation (12), equation (19) can be written as

$$\frac{\partial F}{\partial R}\Theta \cos(R, N) + \frac{1}{R} F \frac{\partial \Theta}{\partial \theta} \cos(\theta, N) = 0, \tag{20}$$

where N represents the outward normal of the duct wall and (a, b) denotes the angle between directions a and b. When θ approaches $\bar{\theta}$, $\cos(R, N)$ and $\cos(\theta, N)$ tend towards 0 and 1 respectively (see Figure 1), so that equation (20) can be reduced to equation (18). Thus, the boundary condition for the characteristic function $\Theta(\theta)$ can be determined by the kinematic condition at $\theta = \bar{\theta}$, i.e., only (18), instead of throughout the duct wall, i.e., (20). Therefore, for various types of the non-uniform portion, the characteristic function $\Theta(\theta)$ can be analytically determined by solving the boundary value problem constituted by equations (14) and (18).

Note that the origin of the spherical co-ordinates is chosen such that $\cos(R, N)$ vanishes at $\theta = \bar{\theta}$ for the boundary condition (20). Otherwise, the boundary condition for $\Theta(\theta)$ is of the following frequency-dependent form

$$\frac{\partial F}{\partial R}\Theta \cos(R, N) + \frac{1}{R} F \frac{\partial \Theta}{\partial \theta} \cos(\theta, N) = 0 \quad \text{at } \theta = \bar{\theta}, \tag{21}$$

instead of the simple frequency-independent equation (18). The frequency-dependent function F (see equations (17) and (15)) contributes to the boundary

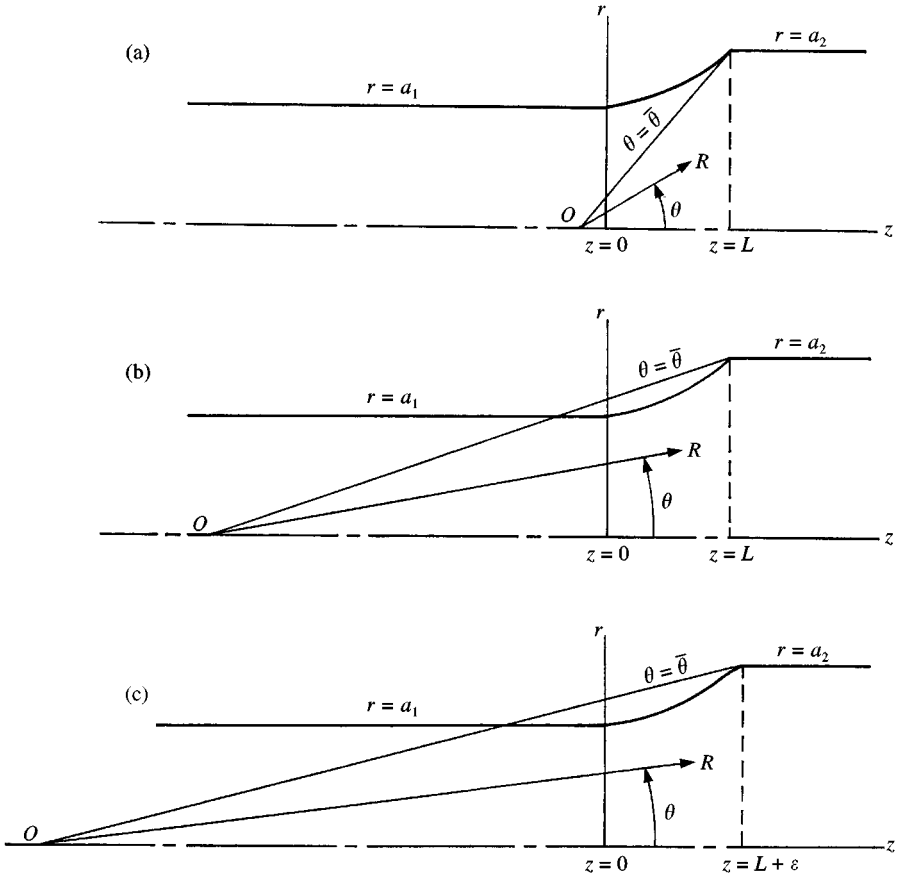

Figure 2. Slight change of duct profile to effect the use of spherical co-ordinates.

condition (21) although the differential equation (14) for $\Theta(\theta)$ is a frequency-independent equation. This requires repeated calculation of the characteristic function $\Theta(\theta)$ for each frequency ω, and consequently increases the computation time and cost.

For the case shown in Figure 2(a), we encounter the problem that the region $0 \leqslant \theta \leqslant \bar{\theta}$ cannot completely absorb the non-uniform portion. If we alter the spherical co-ordinates to solve the problem as shown in Figure 2(b), $\cos(R, N)$ takes a non-zero value at $\theta = \bar{\theta}$ rendering the boundary condition (21) frequency-dependent. To overcome these difficulties, a slight change of the duct profile shown in Figure 2(c) is advisable.

The nth characteristic function determined from equations (14) and (18) is given by

$$\Theta_{mn}(\theta) = \sin^m\theta F_{GAUSS}(m - \alpha, \alpha + m + 1, m + 1, (1 - \cos\theta)/2)$$

$$= \sin^m\theta$$

$$\times \left\{ 1 + \sum_{i=1}^{\infty} \frac{(m-\alpha)(m-\alpha+1)\cdots(m-\alpha+i-1)(\alpha+m+1)(\alpha+m+2)\cdots(\alpha+m+i)}{1\times 2\times \cdots \times i(m+1)(m+2)\cdots(m+i)} \times \left(\frac{1-\cos\theta}{2}\right)^{i} \right\}. \tag{22}$$

Refer to Appendix A for the derivation of equation (22).

Expressing $\Theta_{mn}(\theta)$ in terms of the Gaussian hypergeometric series, $F_{GAUSS}(a, b, c; x)$ [13] is helpful for examining the convergence of the solution series. The Gaussian hypergeometric series $F_{GAUSS}(a, b, c; x)$ converges for abritrary values of a, b and c, provided that $|x| < 1$ [13]. Hence, solution (22) converges for $0 \leqslant \theta \leqslant \pi$. In the present analysis, we have $0 \leqslant \theta \leqslant \bar{\theta}$, where $\bar{\theta}$ is a small angle, as can be seen from Figure 1. Therefore, the convergence of solution (22) is assured.

By superposing the characteristic functions, the sound pressure in the non-uniform section can be expressed as

$$P = \sum_{n=n_{min}}^{n_{max}} \{A_{1mn}F_{1mn}(R) + A_{2mn}F_{2mn}(R)\}\Theta_{mn}(\theta)\cos m\varphi \mathrm{e}^{\mathrm{i}\omega t}. \tag{23}$$

The solutions in the uniform and non-uniform sections (equations (4)–(6) and (23)) must satisfy the condition that the sound pressure and the particle velocity are continuous at the interface between the uniform and non-uniform portions:

$$p^{(I)} + p^{(R)} = P \quad \text{at } z = 0, \tag{24}$$

$$p^{(T)} = P \quad \text{at } z = L, \tag{25}$$

$$\frac{\partial p^{(I)}}{\partial z} + \frac{\partial p^{(R)}}{\partial z} = \frac{\partial P}{\partial z} \quad \text{at } z = 0, \tag{26}$$

$$\frac{\partial p^{(T)}}{\partial z} = \frac{\partial P}{\partial z} \quad \text{at } z = L. \tag{27}$$

Furthermore, solution (23) must satisfy the boundary condition (19). These conditions can be expressed in the form of the Galerkin method for diverging ducts ($a_1 < a_2$):

$$\int_0^{a_1} (p^{(I)} + p^{(R)} - P)|_{z=0}\, r\mathrm{J}_m(\mu_{1mq}r)\,\mathrm{d}r = 0, \tag{28}$$

$$\int_0^{a_2} (p^{(T)} - P)|_{z=L} r J_m(\mu_{2mq} r)\, dr = 0, \tag{29}$$

$$\int_0^{a_1} \left(\frac{\partial p^{(I)}}{\partial z} + \frac{\partial p^{(R)}}{\partial z} - \frac{\partial P}{\partial z} \right)\Bigg|_{z=0} r J_m(\mu_{2mq} r)\, dr + \int_{a_1}^{a_2} \frac{\partial P}{\partial N} [1 + \{z_w'(r)\}^2]^{1/2} r J_m(\mu_{2mq} r)\, dr = 0, \tag{30}$$

$$\int_0^{a_2} \left(\frac{\partial p^{(T)}}{\partial z} - \frac{\partial P}{\partial z} \right)\Bigg|_{z=L} r J_m(\mu_{2mq} r)\, dr, \tag{31}$$

where $q = n_{min}, \ldots, n_{max}$. The factor multiplied by $\partial P/\partial N$ in equation (30) is necessary for expressing the integration over the side wall $z = z_w(r)$ in terms of the r integral. As can be seen from equation (30), conditions (19) and (26) are combined and the residual is expanded using the complete set formed by $J_m(\mu_{2mq} r)$ $(q = n_{min}, \ldots, n_{max})$. For converging ducts $(a_1 > a_2)$, equations (30) and (31) are replaced by

$$\int_0^{a_1} \left(\frac{\partial p^{(I)}}{\partial z} + \frac{\partial p^{(R)}}{\partial z} - \frac{\partial P}{\partial z} \right)\Bigg|_{z=0} r J_m(\mu_{1mq} r)\, dr = 0, \tag{32}$$

$$\int_0^{a_2} \left(\frac{\partial p^{(T)}}{\partial z} - \frac{\partial P}{\partial z} \right)\Bigg|_{z=L} r J_m(\mu_{1mq} r)\, dr - \int_{a_2}^{a_1} \frac{\partial P}{\partial N} [1 + \{z_w'(r)\}^2]^{1/2} r J_m(\mu_{1mq} r)\, dr = 0. \tag{33}$$

By substituting equations (4)–(6) and (23) into equations (28)–(31), we obtain a system of algebraic homogeneous equations for $C_{1mv}, C_{2mn}, C_{3mn}, A_{1mn}$ and A_{2mn} $(n = n_{min}, \ldots, n_{max})$. By solving this system of equations, we can determine the following reflection coefficient R_{mv} and transmission coefficient T_{mv} for a specified incident mode (m, v):

$$R_{mv} = |C_{2mv}/C_{1mv}|, \tag{34}$$

$$T_{mv} = |C_{3mv}/C_{1mv}|. \tag{35}$$

The dimension of the numerical problem for obtaining a sufficiently converging solution is small due to the orthogonality of the characteristic functions (22), so that the present analysis requires only a small amount of computation time and cost.

3. NUMERICAL EXAMPLES

As a test for the accuracy of the present method, numerical computation was carried out for an identical case given in the reference material [11]. The results obtained

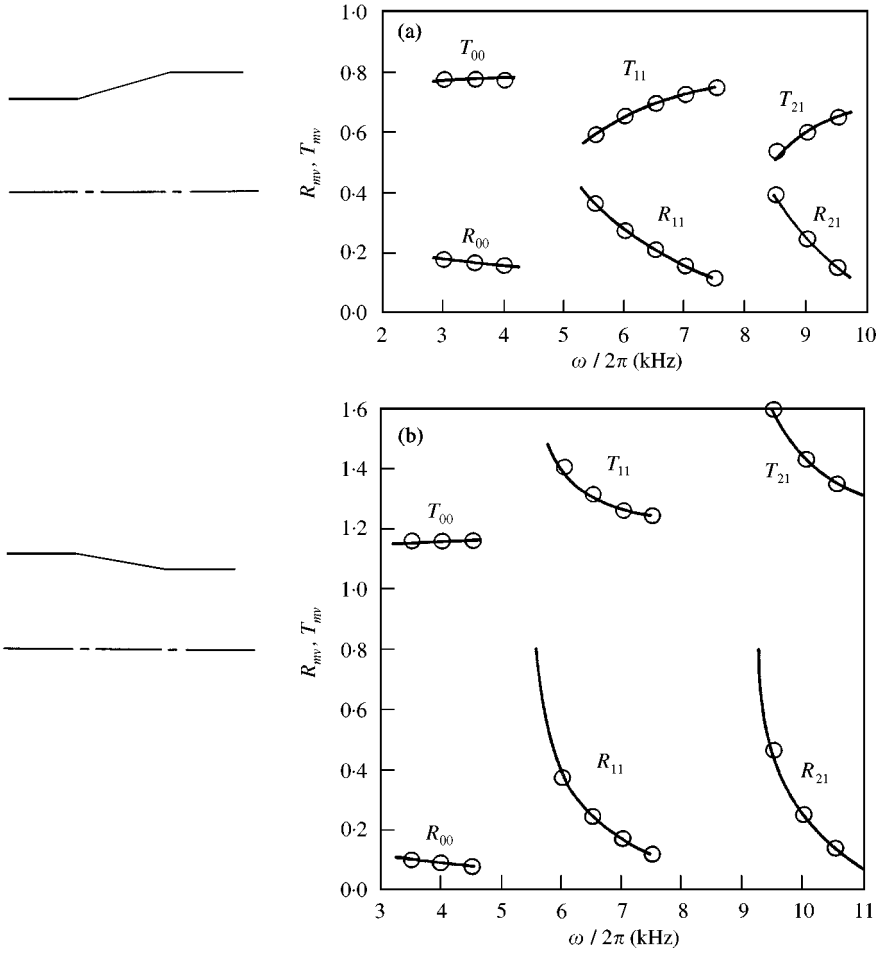

Figure 3. Reflection and transmission coefficients for incident modes $(m, v) = (0, 0), (1, 1)$ and $(2, 1)$; ○, present method; ——, theoretical prediction in the reference material [11]; (a) Diverging linearly tapered transition section with $a_1 = 0{\cdot}0208$ m, $a_2 = 0{\cdot}02645$ m and $L = 0{\cdot}0207$ m. (b) Converging linearly tapered transition section with $a_1 = 0{\cdot}0208$ m, $a_2 = 0{\cdot}01785$ m and $L = 0{\cdot}0207$ m.

by the present method are marked in the figure cited from this reference (Figure 3). Excellent agreement can be confirmed between the results obtained by the present analysis and those of the theoretical prediction in the reference material [11].

The numerical results are shown within the frequency range $\omega \geqslant \max(c\mu_{1mv}, c\mu_{2mv})$, in which the mode (m, v) is an advancing wave in all portions of the duct and hence extremely useful in engineering applications. Below this frequency domain, both or either of the wave numbers k_{1mv} and k_{2mv} is a pure imaginary number, as can be seen from equations (7) and (8), so that the mode (m, v) is unpropagated. The frequencies $c\mu_{1mv}$ and $c\mu_{2mv}$ are the cut-on frequencies [12] for the uniform sections with radii of a_1 and a_2 respectively.

Figure 4 shows the results for the curvilinearly tapered transition section whose side wall profile is given by

$$r = r_w(z) = \tfrac{1}{2}(a_1 + a_2) + A \sin B(z - \tfrac{1}{2}L) \quad (0 \leqslant z \leqslant L), \tag{36}$$

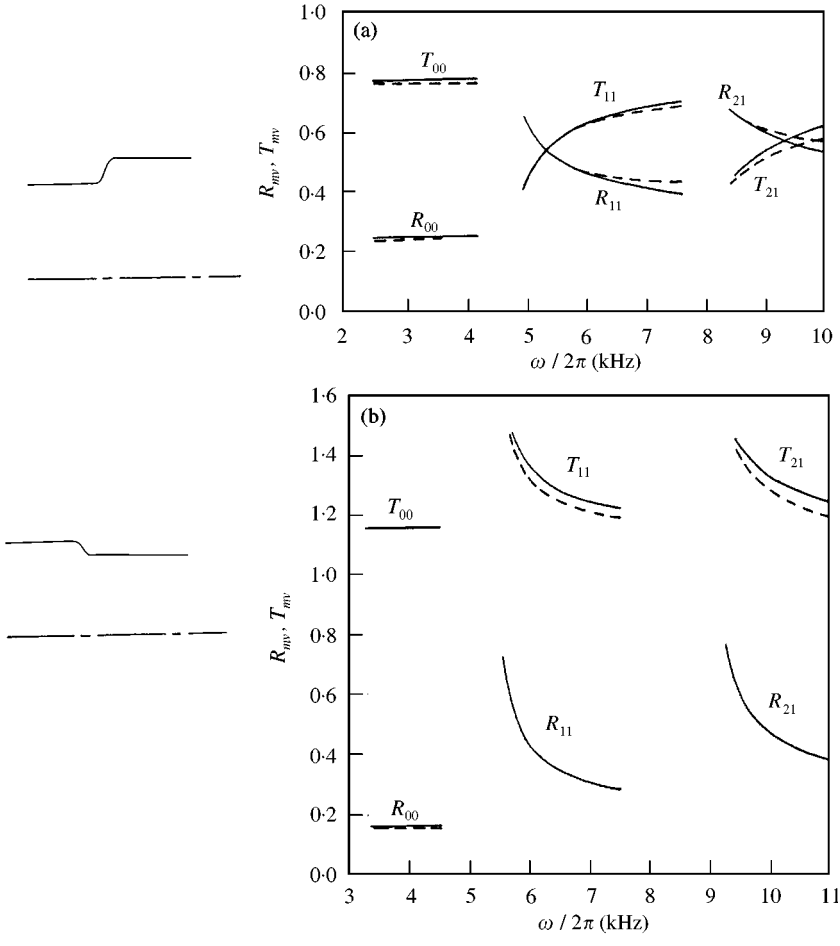

Figure 4. Reflection and transmission coefficients for incident modes $(m, v) = (0, 0), (1, 0)$ and $(2, 1)$; ——, curvilinearly tapered transition section of length $L = 0{\cdot}003$ m; – – –, discontinuous change in cross-section; (a) $a_1 = 0{\cdot}0208$ m, $a_2 = 0{\cdot}02645$ m; (b) $a_1 = 0{\cdot}0208$ m, $a_2 = 0{\cdot}01785$ m.

where the constants A and B are determined by

$$\frac{1}{2}BL = \frac{\pi}{2} \times \frac{7}{9}, \quad A \sin\left(\frac{\pi}{2} \times \frac{7}{9}\right) = \frac{1}{2}(a_2 - a_1). \tag{37}$$

Since the argument of the sine function is equal to -70° and 70° for $z = 0$ and $z = L$ respectively, the geometry of the side wall is represented by the sine curve $A \sin x$ within the range $-70 \leqq x \leqq 70^\circ$. To verify the numerical result, it is compared with the reflection and transmission coefficients for the case in which the radius of the duct discontinuously changes from a_1 to a_2 at $z = 0$. To determine these coefficients, numerical calculation was carried out according to the method presented in the reference material [1], and the results are shown by a dashed line in Figure 4 for the sake of comparison. The same comparison was repeated for the

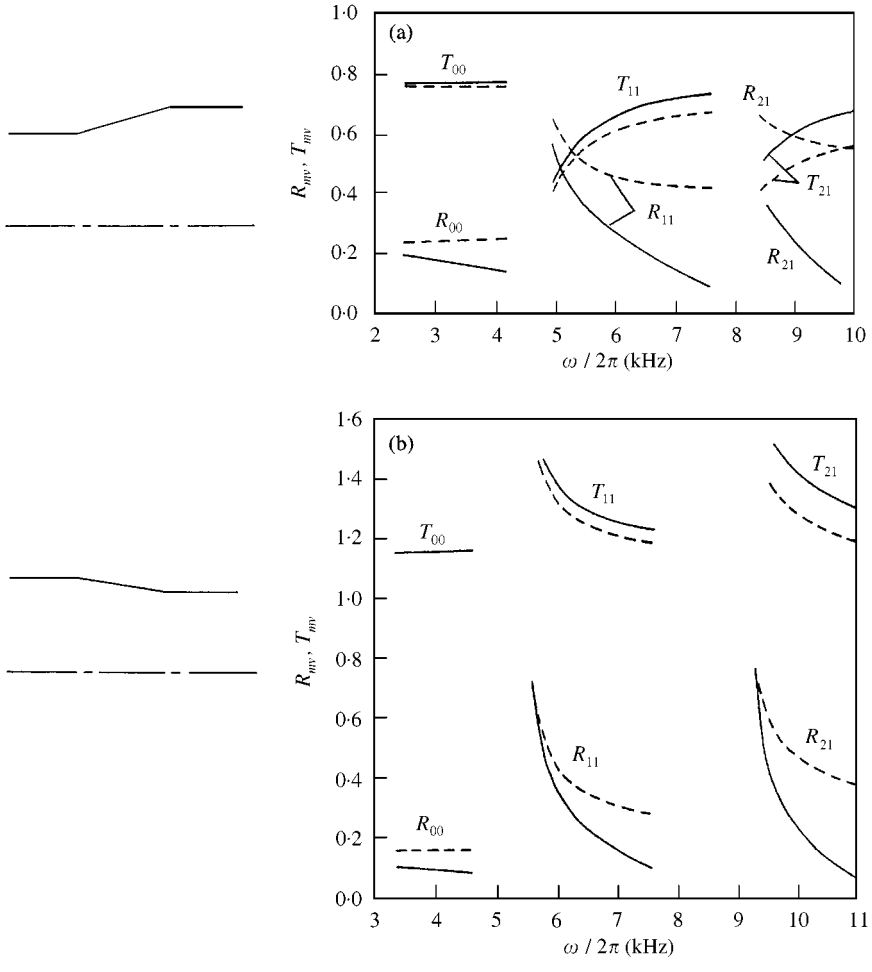

Figure 5. Reflection and transmission coefficients for incident modes $(m, v) = (0, 0), (1, 1)$ and $(2, 1)$; ——, linearly tapered transition section of length $L = 0{\cdot}0207$ m; – – –, discontinuous change in cross-section; (a) $a_1 = 0{\cdot}0208$ m, $a_2 = 0{\cdot}02645$ m; (b) $a_1 = 0{\cdot}0208$ m, $a_2 = 0{\cdot}01785$ m.

linearly tapered transient section formerly employed (Figure 5). For the curvilinearly tapered transient section, the variation in the cross-sectional area is steeper than for the linearly tapered transient section, so that the result should approach the value shown by dashed line to some extent. The curves shown in Figures 4 and 5 indicate the trend. This discussion serves as a verification of the present analysis.

Some significant observations may be made from Figures 4 and 5. First, the difference between the results for the continuous and discontinuous change in cross-sectional area is larger in the case of non-plane wave modes than for the plane wave mode. This signifies that the importance of the present method, which allows for continuous variation in cross-sectional area, is accentuated for the non-plane wave modes of propagation. The second point of interest is that the dependency of the reflection and transmission coefficients on the frequency is much more marked

for the non-plane wave modes than for the plane wave mode. The reflection and transmission coefficients for the non-plane wave modes vary sensitively in the vicinity of the cut-on frequencies of the non-plane modes. A quantitative discussion can be made for this result for the case of the discontinuous change in cross-sectional area. The discussion is useful since the qualitative trend is similar for both continuous and discontinuous change in cross-sectional area. In the case $a_1 < a_2$, for example, the conditions of continuity for the sound pressure and the particle velocity at the interface $z = 0$ are given by

$$\int_0^{a_1} (p^{(I)} + p^{(R)} - p^{(T)})|_{z=0} r \mathrm{J}_m(\mu_{1mq} r)\,\mathrm{d}r = 0, \tag{38}$$

$$\int_0^{a_1} \left(\frac{\partial p^{(I)}}{\partial z} + \frac{\partial p^{(R)}}{\partial z} - \frac{\partial p^{(T)}}{\partial z} \right)\Bigg|_{z=0} r \mathrm{J}_m(\mu_{2mq} r)\,\mathrm{d}r - \int_{a_1}^{a_2} \frac{\partial p^{(T)}}{\partial z}\Bigg|_{z=0} r \mathrm{J}_m(\mu_{2mq})\,\mathrm{d}r = 0. \tag{39}$$

Using the assured approximation that the mode $n = v$ is predominant for the reflected and transmitted waves and substituting equations (4)–(6) into equations (38) and (39) yield

$$S_{11mv} C_{2mv} - S_{12mv} C_{3mv} = - S_{11mv} C_{1mv}, \tag{40}$$

$$\mathrm{i} k_{1mv} S_{12mv} C_{2mv} + \mathrm{i} k_{2mv} S_{22mv} C_{3mv} = \mathrm{i} k_{1mv} S_{12mv} C_{1mv} \tag{41}$$

with

$$S_{ijmv} = \int_0^{\alpha} r \mathrm{J}_m(\mu_{imv} r) \mathrm{J}_m(\mu_{jmv} r)\,\mathrm{d}r, \tag{42}$$

where $\alpha = a_2$ for $(i, j) = (2, 2)$ and $\alpha = a_1$ otherwise. Solving equations (40) and (41), we determine the reflection and transmission coefficients as

$$\begin{Bmatrix} R_{mv} \\ T_{mv} \end{Bmatrix} =$$

$$\begin{Bmatrix} C_{2mv}/C_{1mv} \\ C_{3mv}/C_{1mv} \end{Bmatrix} = \frac{1}{k_{1mv} S_{12mv}^2 + k_{2mv} S_{11mv} S_{22mv}} \begin{Bmatrix} k_{1mv} S_{12mv}^2 - k_{2mv} S_{11mv} S_{22mv} \\ 2 k_{1mv} S_{11mv} S_{12mv} \end{Bmatrix}. \tag{43}$$

For the plane wave mode $(m, v) = (0, 0)$, as can be seen from equations (7), (8) and (10), the angular frequency ω in the denominator and the numerator in equation (43) cancel out, so that the reflection and transmission coefficients are reduced to constants. For the non-plane wave modes, on the other hand, these coefficients vary sensitively near the cut-on frequencies. When the frequency is increased from the cut-on frequency of each non-plane wave mode, the values in the

brace brackets in equations (7) and (8) have their first terms to prevail, so that the dependency of the reflection and transmission coefficients on the frequency becomes less marked. (For the plane wave mode, the second terms are exactly zero, as can be seen from equation (10)).

4. CONCLUSION

The reflection and transmission coefficients of acoustic waves in ducts at the location of a continuous variation in cross-sectional area have been calculated for the non-plane wave modes as well as the plane wave mode. The solution method and numerical results can be characterized as follows.

1. The use of spherical co-ordinates enable us to determine analytically the system of characteristic functions for various profiles of the non-uniform portion. The system of characteristic function can be used as a complete set to express the solution over the non-uniform region. Since the dimension of the resulting numerical problem is low, the present analysis requires little computation time and cost.
2. The difference between the results for the continuous and the discontinuous changes in cross-sectional area is larger for the non-plane wave modes than for the plane wave mode. This signifies that the importance of the present method, which allows for continuous variation in cross-sectional area, is accentuated for the non-plane wave modes of propagation.
3. The dependence of the reflection and transmission coefficients on the frequency is more marked for the non-plane wave modes than for the plane wave mode.

REFERENCES

1. J. Miles 1944 *Journal of the Acoustical Society of America* **16**, 14–19. The reflection of sound due to a change in cross section of a circular tube.
2. W. Eversman, E. L. Cook and R. J. Beckemeyer 1975 *Journal of Sound and Vibration* **38**, 105–123. A method of weighted residuals for the investigation of sound transmission in non-uniform ducts without flow.
3. P. T. Vo and W. Eversman 1978 *Journal of Sound and Vibration* **56**, 243–250. A method of weighted residuals with trigonometric basis functions for sound transmission in circular ducts.
4. W. Eversman and R. J. Astley 1981 *Journal of Sound and Vibration* **74**, 89–101. Acoustic transmission in non-uniform ducts with mean flow. Part I: the method of weighted residuals.
5. R. J. Astley and W. Eversman 1978 *Journal of Sound and Vibration* **57**, 367–388. A finite element method for transmission in non-uniform ducts without flow: comparison with the method of weighted residuals.
6. R. J. Astley and W. Eversman 1981 *Journal of Sound and Vibration* **74**, 103–121. Acoustic transmission in non-uniform ducts with mean flow. Part II: the finite element method.
7. A. H. Nayfeh, J. E. Kaiser, R. L. Marshall and C. J. Hurst 1980 *Journal of Sound and Vibration* **71**, 241–259. A comparison of experiment and theory for sound propagation in variable area ducts.

8. C. K. W. Tam 1971 *Journal of Sound and Vibration* **18**, 339–351. Transmission of spinning acoustic modes in a slightly non-uniform duct.
9. W. E. Zorumski and L. R. Clark 1971 *Unpublished Working Paper, NASA Langley Research Center*. Sound radiation from a source in an acoustically treated circular duct.
10. R. J. Alfredson 1972 *Journal of Sound and Vibration* **23**, 433–442. The propagation of sound in a circular duct of continuously varying cross-sectional area.
11. A. Sadamoto, Y. Murakami and S. Masuda 1993 *Journal of Acoustical Society of Japan* **49**, 235–242. Calculation for reflection and transmission of higher-order mode sound waves at sections of varying cross-sectional area in circular ducts (in Japanese).
12. L. J. Eriksson 1980 *Journal of the Acoustical Society of America* **68**, 545–550. Higher order mode effects in circular ducts and expansion chambers.
13. Horace Lamb 1879 *Hydrodynamics*, p. 113. London: Cambridge University Press, seventh edition, 1975.

APPENDIX A: DERIVATION OF EQUATION (22)

The new variables

$$\xi = \cos\theta, \quad u(\xi) = (1 - \xi^2)^{-m/2}\Theta(\theta) \tag{A1}$$

transform equation (14) to

$$\frac{\mathrm{d}^2u}{\mathrm{d}\xi^2} - \frac{2(m+1)\xi}{1-\xi^2}\frac{\mathrm{d}u}{\mathrm{d}\xi} + \frac{\lambda - m(m+1)}{1-\xi^2}u = 0 \tag{A2}$$

which can be solved using power-series expansion. Substituting

$$u(\xi) = (\xi - 1)^\rho \sum_{i=0}^{\infty} a_i(\xi - 1)^i \tag{A3}$$

into equation (A2), one obtains an equation for ρ, namely

$$\rho(\rho + m) = 0 \tag{A4}$$

and a recurrence relation for the coefficients a_i:

$$a_{i+1} = \frac{\lambda - i(i+1) - m(m+1+2i)}{2(i+1)(i+1+m)}a_i. \tag{A5}$$

Equation (A4) admits $\rho = 0$ for the bounded solution at $\xi = 1$ ($\theta = 0$). The characteristic values $\lambda = \lambda_{mn}$ ($n = 1, 2, \ldots$) must be determined such that the solution (A3) satisfies the boundary condition (18). By introducing a parameter α satisfying $\alpha(\alpha + 1) = \lambda$, equation (A5) can be transformed into

$$a_{i+1} = \frac{-(m - \alpha + i)(\alpha + m + i + 1)}{2(i+1)(m+i+1)}a_i \tag{A6}$$

using which the required characteristic function can be expressed in terms of the Guassian hypergeometric series as equation (22).